Gravitational Lens Statistics and The Density Profile of Dark Halos

Ryuichi Takahashi and Takeshi Chiba
Department of Physics, Kyoto University, Kyoto 606-8502, Japan

ABSTRACT

We investigate the influence of the inner profile of lens objects on gravitational lens statistics taking into account of the effect of magnification bias and both the evolution and the scatter of halo profiles. We take the dark halos as the lens objects and consider the following three models for the density profile of dark halos; SIS (singular isothermal sphere), the NFW (Navarro Frenk White) profile, and the generalized NFW profile which has a different slope at smaller radii. The mass function of dark halos is assumed to be given by the Press-Schechter function. We find that magnification bias for the NFW profile is order of magnitude larger than that for SIS. We estimate the sensitivity of the lensing probability of distant sources to the inner profile of lenses and to the cosmological parameters. It turns out that the lensing probability is strongly dependent on the inner density profile as well as on the cosmological constant. We compare the predictions with the largest observational sample, the Cosmic Lens All-Sky Survey. The absence or presence of large splitting events in larger surveys currently underway such as the 2dF and SDSS could set constraints on the inner density profile of dark halos.

Subject headings: cosmology: gravitational lensing — dark matter:clusters

1. Introduction

It has been known since the 1930s that dark matter is the gravitationally main component in a variety of astrophysical objects such as galaxies and clusters of galaxies, but the nature of dark matter still eludes us. (Peebles 1993). Recently, the systematic discrepancy between numerical simulations and observations regarding the inner density profile of dark halos has been reported. For the inner density profile of dark halos $\rho(r) \propto r^{-\alpha}$, numerical simulations suggest the steeper profile $\alpha \sim 1 - 1.5$, while observations suggest the shallower profile $\alpha \sim 0 - 1$. Numerical simulations of CDM halos by Navarro, Frenk & White

(1996,1997, hereafter NFW) have shown that the density profile has the "universal" form $\rho \propto r^{-1}(r+r_s)^{-2}$, where r_s is the scale length, irrespective of the cosmological parameters, the initial power spectrum and the formation histories. Following NFW, higher-resolution simulations have been performed, and the results suggest the steeper inner slope $\rho(r) \propto r^{-1.5}$ (Moore *et al.* 1999, Fukushige & Makino 2001). On the other hand, observations of rotation curves of the spiral and the low surface brightness galaxies indicate the shallower halo profile $\alpha \sim 0-1$ (van den Bosch *et al.* 2000, de Blok *et al.* 2001, Borriello & Salucci 2001). The mass distribution of the cluster CL0024+1654 is reconstructed from lensed images and indicates the flat core (Tyson *et al.* 1998). It is important to resolve the discrepancy to get clues to the nature of dark matter.

In this regard, strong gravitational lensing effects can provide an important method to probe the nature of dark matter. Strong lensing probes the inner dense region of lens objects, and the impact parameter is estimated as

$$\xi \simeq 6.2\ {h_{70}}^{-1}\ \ \mathrm{kpc}\ \frac{H_0 D_L}{0.3}\frac{\theta}{1''}, \tag{1}$$

where D_L is the distance to the lens and θ is the image separation. So it is sensitive to the inner profile of lenses and can be a useful method for probing the inner profile of dark halos. In fact, ξ in Eq.(1) is comparable to the scale length r_s in the NFW profile $\rho \propto r^{-1}(r+r_s)^{-2}$ (Navarro, Frenk & White 1997). Dark halos is gravitationally dominant in galactic halos and clusters of galaxies. However, at the inner region of galaxies, baryonic components such as bulge and disk are also gravitationally dominant, and dissipation processes among the baryons are important. On the other hand, since clusters of galaxies are formed only recently, the baryonic component distributes broadly as gas (Rees & Ostriker 1977) and the radial distribution of gas mass is similar to the total mass (Einasto & Einasto 2000). Hence, in order to study strong gravitational lensing without the need to include the gravitational effects of baryonic components, we shall mainly concentrate on clusters of galaxies as the lens objects and look for large-separation images (the effect of baryons on lensing was studied in (Porciani & Madau 2000, Kochanek & White 2001, Keeton 2001)).

In this paper, we examine the effect of the inner density profile of lens objects on gravitational lens statistics, including the effect of magnification bias and both the evolution and the scatter of halo profiles. Statistics of gravitational lensing of QSOs provides a useful tool to set constraints on the cosmological constant (Fukugita *et al.* 1992, Kochanek 1996). However, it depends on the lens model such as the profile of lenses and its number density as well as cosmology. Hence, in using it as a tool to limit the cosmological constant, we must be careful about the uncertainties concerning the lens model. We estimate the sensitivity of the lensing probability of distant sources to the inner profile of lenses and to the cosmological constant. We consider three kinds of density profile of lens objects : SIS ($\rho(r) \propto r^{-2}$), the

NFW ($\rho(r) \propto r^{-1}$ for the inner profile), the generalized NFW ($\rho(r) \propto r^{-\alpha}$ for the inner profile). Only smooth and spherical models are considered. Subclumps (cluster galaxies) in clusters do not affect the cross section of lensing (Flores *et al.* 2000). Nonsphericity can affect the relative frequency of four-image lenses (Rusin & Tegmark 2001). The distribution of lenses is taken to be the Press-Schechter function. We compare the predictions with the large observational data, CLASS (the Cosmic Lens All-Sky Survey), and predict for larger surveys such as 2dF and SDSS. Multiple images of large separation angles are expected to be caused by clusters of galaxies, so when we compare the observational data, we will use the large angle images ($\theta \geq 6''$). The statistics of wide-separation lenses ($\xi \geq 10$kpc) has been used to probe the distributions of mass inhomogeneities derived from the CDM scenarios, since one does not need to be concerned with the physics of baryonic components and bias (Wambsganss *et al.* 1995). By studying the lensing properties in this regime assuming the CDM scenarios, theoretical calculations based on N-body simulations (Cen *et al.* 1994, Wambsganss *et al.* 1995, Wambsganss *et al.* 1998) and semi-analytical method using the Press-Schechter function (Narayan & White 1988, Kochanek 1995, Nakamura & Suto 1997, Mortlock & Webster 2000) have been used to place limits on cosmological parameters. Similarly, incorporating realistic input for mass profile and number density of clusters, analytical calculations have been used to set constraint to cosmological models (Tomita 1996) and lens models (Maoz *et al.* 1997). We pay particular attention to the influence of the inner lens structure on the statistics of wide-separation lenses (for earlier discussion before NFW profile, see Flores & Primack 1996).

Recently a similar analysis has been performed by several authors (Wyithe, Turner & Spergel 2000, Fox & Pen 2001, Li & Ostriker 2000, Keeton & Madau 2001). Wyithe, Turner & Spergel (2001) used the generalized NFW lens model and suggested the optical depth to multiple imaging of the distant sources is very sensitive to the inner lens profile, but no comparison with observational data was made. Li & Ostriker (2000) found that the lensing probability is very sensitive to the density profile of lenses, and somewhat less so to the cosmological parameters such as the mean mass density in the universe and the amplitude of primordial fluctuations. However, they did not take into account the scatter of dark halo profiles (concentration parameter) and the uncertainty in the treatment of magnification bias. Keeton & Madau (2001) found that the number of predicted lenses is strongly correlated with the core mass fraction. In this paper, we present a systematic study of the effect of the inner dark halo profile and cosmological parameters on gravitational lens statistics. It is very important to be careful about both the effect of magnification bias, which depends on the lens profile and magnification of each images, and both the evolution and the scatter of halo profiles in N-body simulations (Bullock *et al.* 2001).

This paper is organized as follows. In section 2, we briefly summarize the basic formulae

of gravitational lens statistics for various lens models. In section 3, we examine the effect of magnification bias and compare the theoretical prediction with observation. In section 4, we estimate the number of lensed images expected in larger surveys. Finally, in section 5, we summarize the main results of this paper. We use the units of $c = G = 1$.

2. Basics

2.1. SIS Lens

The SIS (singular isothermal sphere) model is frequently used in the lensing analysis, since it is supported by observed flat rotation curves and moreover the density profile is very simple and quantities related to gravitational lensing can be written in simple analytic forms (Turner, Ostriker & Gott 1984). SIS is characterized by the one-dimensional velocity dispersion v, and the density profile is $\rho(r) = v^2/2\pi r^2$. The lens equation leads to the two solutions (image positions) at $x_\pm = y \pm 1$ with magnifications $\mu_\pm = |(y/x_\pm)(dy/dx_\pm)|^{-1} = 1/y \pm 1$, where dimensionless quantities x and y are the impact parameter divided by the Einstein radius in the lens plane and the source position divided by it in the source plane (Schneider, Ehlers & Falco 1992). Magnification of the brighter (fainter) image is $\mu_+(\mu_-)$, and the total magnification is $\mu(y) = 2/y$. The splitting angle between the two images is $\theta = 8\pi v^2 D_{LS}/D_S$, where D_L, D_S and D_{LS} are the angular diameter distances between the observer, lens and source. We shall adopt the so-called filled beam distance (Dyer & Roeder 1973), since the ray shooting in an inhomogeneous universe created by N-body simulations is consistent with it (Tomita 1998, Tomita, Asada & Hamana 1999).

When the light ray from the source passes near the lens object, if $|y| \leq 1$, double images form. We define the cross section $\sigma(v, z_L, z_S)$ as the area of a region in the source plane which satisfies the following criteria; (i)double images are formed, and (ii)the magnification is larger than the minimum amplification μ_*. The second condition is needed for the calculation of magnification bias (see Eq.(15) below). Then, the cross section is given by,

$$\sigma(v, z_L, z_S) = \pi r_E^2 \times 2 \int_0^1 dy y \Theta(\mu(y) - \mu_*), \tag{2}$$

where $r_E (= 4\pi v^2 D_{LS})$ is the Einstein radius in the source plane, and $\Theta(x)$ is the step function.

2.2. Generalized NFW Lens

In this section we consider the generalized NFW profile for dark halos (Wyithe, Turner & Spergel 2000, Li & Ostriker 2000),

$$\rho(r) = \frac{\rho_s}{\left(\frac{r}{r_s}\right)^{\alpha}\left(\frac{r}{r_s}+1\right)^{3-\alpha}}, \tag{3}$$

where ρ_s and r_s are parameters which depend on the mass of halo M and redshift z, and $\alpha(0 \leq \alpha \leq 2)$ is a constant. The scale radius r_s is about 10 kpc on a galactic halo scale ($M \sim 10^{12} M_\odot$) and 100 kpc on a cluster scale ($M \sim 10^{15} M_\odot$) (Navarro, Frenk & White 1997). Since the impact parameter ξ is comparable to the scale radius r_s (see Eq.(1)), we could set a strong constraint on inner slope α in Eq.(3) by using strong gravitational lensing. We consider the case of $\alpha = 0.5, 1, 1.5$.

The concentration parameter c and the characteristic density δ_c are respectively defined by

$$c = \frac{r_{vir}}{r_s}, \tag{4}$$

$$\delta_c = \frac{\rho_s}{\rho_m(z)} = \frac{\Delta_{vir}}{3}\frac{c^3}{\int_0^c dx\ x^{2-\alpha}(1+x)^{\alpha-3}}. \tag{5}$$

c represents degree of the mass concentration at the inner region of a halo. The virial radius of the halo r_{vir} is related to the mass M and redshift z as

$$H_0 r_{vir} = 5.643 \times 10^{-5} h^{1/3} \Omega_0^{-1/3} (1+z)^{-1} \left(\frac{\Delta_{vir}}{18\pi^2}\right)^{-1/3} \left(\frac{M}{10^{12} M_\odot}\right)^{1/3}, \tag{6}$$

where Δ_{vir} is the overdensity of the halo ($\Delta_{vir} = 18\pi^2$ for EdS ($\Omega_0 = 1$) model, and for other cosmological models we use the fitting formulae given in Kitayama & Suto 1996 and Nakamura & Suto 1997).

For the NFW profile ($\alpha = 1$), c is fitted by the numerical simulation (Navarro, Frenk & White 1997). For the generalized NFW profile, following the recent work (Bullock *et al.* 2001, Keeton & Madau 2001), we define c to be $c = r_{vir}/r_{-2}$, where r_{-2} is the radius at which the logarithmic slope of the density profile is -2 (r_{-2} is equivalent to r_s for the NFW profile). Thus we obtain $c = (2-\alpha)^{-1} r_{vir}/r_s$.

However, there is a scatter in the concentration parameter c at fixed mass and redshift (Bullock *et al.* 2001, Jing 2000). Keeton & Madau (2001) pointed out the importance of the scatter of c on the lensing statistics. We adopt a log-normal function as the probability

distribution function of c,

$$p(c)dc = \frac{1}{\sqrt{2\pi}\sigma_c} \exp\left[-\frac{(\ln c - \ln c_{med})^2}{2\sigma_c^2}\right] d\ln c, \tag{7}$$

with $\sigma_c = 0.18$ (Bullock *et al.* 2001, Jing 2000).

Using the toy model of a $c_{med} - M$ relation found by Bullock *et al.* (2001), we estimate the concentration of the halos,

$$c_{med} = \frac{10}{1+z}\left(\frac{M}{M_*}\right)^{-\beta}, \tag{8}$$

where the fitting parameters (M_*, β) are $(7.0 \times 10^{13} M_\odot, 0.16)$ for EdS $(h = 0.5, \Omega_0 = 1, \lambda_0 = 0, \sigma_8 = 0.67)$ model, $(2.1 \times 10^{13} M_\odot, 0.14)$ for Λ $(h = 0.7, \Omega_0 = 0.3, \lambda_0 = 0.7, \sigma_8 = 1)$ model and $(2.6 \times 10^{13} M_\odot, 0.19)$ for open $(h = 0.7, \Omega_0 = 0.3, \lambda_0 = 0, \sigma_8 = 0.85)$ model. Recent high resolution numerical simulations (Bullock *et al.* 2001) show that c does depend on z contrary to the earlier suspicious that c does not vary much with the redshift (Navarro, Frenk & White 1997).

The lens equation for the halo with the generalized NFW profile is

$$y = x - A\ \frac{g(x)}{x} \tag{9}$$

where $x = \xi/r_s$ (ξ is the impact parameter in the lens plane), $y = (D_L/D_S)(\eta/r_s)$ (η is source position in the source plane), and

$$g(x) = \int_0^x dz\ z^{2-\alpha} \int_0^{\pi/2} d\theta\ \frac{\cos\theta}{(\cos\theta + z)^{3-\alpha}}, \tag{10}$$

$$A = 16\pi\ \rho_s\ \frac{D_L D_{LS}}{D_S}\ r_s. \tag{11}$$

For $\alpha = 0, 1, 2$, the integration of the Eq.(10) can be carried out analytically (the lens equation for the NFW lens was obtained by Bartelmann (1996)). In Fig.2, we show the lens equation for the NFW lens with $A = 10$. If $|y| \leq y_{crit}$, three images x_i $(i = 1, 2, 3, x_3 \geq x_2 \geq x_1)$ form. The image positions $x_i = x_i(y)$ with magnifications $\mu_i(y)$ can be obtained numerically. The image separation angle θ is defined as the separation between the outer two images and depends on the source position y. We use the averaged value in the source plane.

$$\theta(M, z_L) = \frac{1}{\pi y_{crit}^2} \int_0^{y_{crit}} d(\pi y^2)(x_3 - x_1)\frac{r_s(M, z_L)}{D_L}. \tag{12}$$

The total magnification is the sum of the magnifications of three images ($\sum_{i=1}^{3}\mu_i$) and the magnification of the fainter image is smaller magnification of outer two images (min $\{\ \mu_1, \mu_3\ \}$). Following the case of SIS (see Eq.(2)), the cross section is defined by

$$\sigma(M, z_L, z_S) = \pi\ \left(\frac{D_S}{D_L} r_s\right)^2 \times 2\int_0^{y_{crit}} dy y\ \Theta(\mu(y) - \mu_*). \tag{13}$$

2.3. Lensing Probability

The lensing probability for a source at redshift z_S is (Schneider, Ehlers & Falco 1992)

$$P(z_S) = \int_0^{\infty} dM \int_0^{z_S} dz_L\ \frac{1}{{D_S}^2}\ \frac{(1+z_L)^2}{H(z_L)} {D_L}^2\ \sigma(M, z_L, z_S)\ N_M(M, z_L), \tag{14}$$

where $H(z) = H_0\,[\ \Omega_0(1+z)^3 + (1-\Omega_0-\lambda_0)(1+z)^2 + \lambda_0\ ]^{1/2}$ is the Hubble parameter at redshift z, and $N_M(M, z_L)$ is the comoving number density of lenses and is assumed to be given by the Press-Schechter mass function. The one-dimensional velocity dispersion v is related to the mass through $v = (M/2r_{vir})^{1/2}$, and this relates the PS mass function to the SIS lens profile. The probability of the image separation angle is obtained by computing $dP/d\theta$.

Since gravitational lensing causes a magnification of images, lensed sources are over-represented in a magnitude-limited sample and the actual lensing probability is enhanced. This selection effect is called magnification bias. Let $\Phi_S(z_S, L)\ dL$ be the luminosity function of sources. The observed flux S for a lensed source is related to the luminosity L, $L = 4\pi(1+z_S)^4\ D_S^2\ (1+z_S)^{\gamma-1} S$, where the factor $(1+z_S)^{\gamma-1}$ is the K-correction, which assumes that the energy spectrum of source is of the form $E \propto \nu^{-\gamma}$. When one searches for lensed source of the observed flux S, the lensing probability increases as

$$P^B(z_S, L) = \frac{1}{\Phi_S(z_S, L)} \int_1^{\infty} d\mu_*\ \left|\frac{d}{d\mu_*} P(z_S)\right|\ \Phi_S(z_S, L/\mu_*)\ 1/\mu_*. \tag{15}$$

Including magnification bias, the lensing probability $P^B(z_S, L)$ for the generalized NFW lens is expressed as Eq.(14) with $\sigma(M, z_L, z_S)$ replaced by

$$\sigma^B(M, z_L, z_S, L) = \pi\ \left(\frac{D_S}{D_L} r_s\right)^2 \times\ \frac{2}{\Phi_S(z_S, L)} \int_0^{y_{crit}} dy\ y\ \Phi_S(z_S, L/\mu(y))/\mu(y). \tag{16}$$

$\mu(y)$ can be the magnification of the total images or the fainter image. We will discuss each case in Sec. 3.1.

2.4. Press-Schechter Function

We use the Press-Schechter (PS) function (Press & Schechter 1974) for computing the number density of the halos. The PS mass function is given by

$$N_M(M,z)\ dM = \sqrt{\frac{2}{\pi}}\ \frac{\rho_0}{M}\ \frac{\delta_{crit}(z)}{\sigma(R)}\ \left|\frac{d\ln\sigma}{d\ln M}\right|\ \exp\left[-\frac{\delta_{crit}^2(z)}{2\sigma^2(R)}\right]\ \frac{dM}{M}. \tag{17}$$

Here ρ_0 is the mean mass density of the universe at present and $\sigma(R)$ is the linear density fluctuation presently on the comoving scale R,

$$\sigma^2(R) = \frac{1}{2\pi^2}\int_0^\infty dk\ k^2\ P(k)\ W^2(kR)\ , \quad R = \left(\frac{2M}{\Omega_0 {H_0}^2}\right)^{1/3}, \tag{18}$$

where $P(k)$ and $W(kR)$ are the power spectrum at present (Bardeen *et al.* 1986, Sugiyama 1995) and the top-hat window function. We normalize $\sigma(R)$ so that $\sigma(R = 8h^{-1}\mathrm{Mpc}) = \sigma_8$, and the critical density contrast is $\delta_{crit}(z) = 1.686/D_1(z)$, where $D_1(z)$ is the linear growth rate normalized to unity at $z = 0$.

3. Results

In order to explore the dependence of the lensing probability on cosmological models, we consider three representative models; EdS model ($h = 0.5, \Omega_0 = 1, \lambda_0 = 0, \sigma_8 = 0.67$), Λ model ($h = 0.7, \Omega_0 = 0.3, \lambda_0 = 0.7, \sigma_8 = 1$), open model ($h = 0.7, \Omega_0 = 0.3, \lambda_0 = 0, \sigma_8 = 0.85$).

3.1. The Effect of Magnification Bias

We demonstrate the effect of magnification bias by calculating the biased lensing probability Eq.(14, 15). In calculating magnification bias, we use an optical QSO luminosity function. We adopt the 2dF QSO redshift survey data which include about 6000 QSOs with the redshift distribution $0.35 < z < 2.3$ (Boyle *et al.* 2000). The QSO luminosity function is fitted by the two-power-law model

$$\Phi_S(z_S, L)dL = \frac{\Phi_S^*\ dL}{(L/L_*)^{c_1} + (L/L_*)^{c_2}}, \tag{19}$$

$$L_*(z_S) = L_{0*}10^{k_1 z_S + k_2 z_S^2}. \tag{20}$$

The fitting parameters for Λ model are given by

$$(c_1, c_2, M_{B*}, k_1, k_2) = (3.41, 1.58, -21.14 + 5\log h, 1.36, -0.27), \quad (21)$$

$$\Phi_S^* = 2.88 \times 10^{-6} h^3 \mathrm{Mpc}^{-3} \mathrm{mag}^{-1}, \quad (22)$$

where M_{B*} is the absolute B-band magnitude corresponding to L_{0*} (Eq.(20)). We take the absolute magnitude of a source is $M_B = -25.8$ mag in Eq.(20) and consider the image separation range $\theta \geq 0.3''$. For the energy spectrum index of source (see section 2.3), we use $\gamma = 0.5$ for the optical QSOs (Boyle *et al.* 1988). In Fig.2, the effect of magnification bias for SIS and the NFW is shown for Λ model. The vertical axis is the lensing probability with magnification bias divided by that without it. As the source redshift is higher, the amplitude of magnification bias is smaller. This is because the number of fainter QSOs (its luminosity is $L \leq L_*$) is smaller at higher redshift (Eq.(19)), so the integration of luminosity function Eq.(16) takes a smaller value. From Fig.2, we find that the magnification bias effect for the NFW is order of magnitude larger than that for SIS. This is due to the fact that the magnification for the NFW is divergent at $y = y_{crit}$ and $y = 0$ (see Fig.2). Hence, if we attempt to predict lensing frequencies by using the NFW lens model, magnification bias should not be ignored.

In Fig.2, we also compare the case when μ in Eq.(16) is the magnification of the total images with the case of the fainter image. Depending on the properties the gravitational lensing configuration, we should use μ in the bias factor as the magnification of the total images (we call "μ total") or the fainter image among the outer two images ("μ fainter"). If individual sources in a sample are not examined closely enough to determine whether they are lensed or not, the magnification of the fainter image should be used (Sasaki & Takahara 1993, Cen *et al.* 1994) because the fainter image should be bright enough to be recognized as one of the multiple images. On the contrary, if one searches for lensed source of small separation angles, then the total magnification may be relevant, because it is likely that the brightness of a lensed source with a small separation is recognized as the total brightness of all the images. So as far as images of large separation angles are concerned, it may be better to use μ as the magnification of the fainter image.

From Fig.2, different choice of μ in the bias factor greatly changes the amplitude of magnification bias for SIS, but does not change it so much for the NFW; the difference is only factor of three. This is because the magnification for the NFW is divergent at $y = 0$ more strongly than at $y = y_{crit}$ and the magnifications of both of the outer two images (including the fainter image) are divergent at $y = 0$ (see Fig.1). In the following we will consider both cases (μ total or μ fainter), since the degree of the magnification bias depends on the method of gravitational lensing search and thus the expected number of lensed sources will be in between.

3.2. Comparison with the CLASS Data

In this section, we compare predicted lens statistics with a well-defined observational sample. The Cosmic Lens All-Sky Survey (CLASS) is the largest statistically homogeneous search for gravitational lenses (Browne & Myers 2000). The sample comprises 10,499 flat-spectrum radio sources with flux $S > 30$ mJy at 5 GHz, and includes 18 gravitational lenses with image separations $0.3'' \leq \theta \leq 6.0''$. An explicit search for lenses with image separations $6.0'' \leq \theta \leq 15.0''$ has found no lenses (Phillips *et al.* 2000). The flux distribution of flat-spectrum radio sources in the CLASS samples can be described as a power-law (Rusin & Tegmark 2001)

$$\Phi_S(z_S, L)dL \propto L^{-2.1}dL. \tag{23}$$

It is a steeper number-flux relation than predicted by the Dunlop & Peacock (1990) luminosity function (whose slope is -1.8 for the faint sources). The redshift distribution of the full CLASS sample is not known. Marlow *et al.* (2000) reported the redshifts for a small subsample of 27 sources. We assume that the redshift distribution of the full sample is identical to that of the subsample. We need not consider the magnitude distribution of the sample, since the lensing probability does not depend on the magnitude of the source for the power-law luminosity function.

In Fig.3-5, we show the predicted image separation distribution of expected number of lensed source's in the CLASS with magnification bias for each case of μ. The angular resolution of parent survey in the CLASS is very low. The survey flux encompasses all the flux of even the widest separation lenses observed to date. The CLASS survey then reimages the systems looking for multiple imaging (Myers *et al.* 1995, Mortlock & Webster 2000, Helbig 2000). Hence, for the lensed source, μ is given by summing the fluxes of all images (i.e. "μ total" is appropriate). In these figures, we also show the case of "μ fainter " for comparison. We note that the lenses of large separation angle ($\theta \geq 6''$) is expected to be lensed by clusters of galaxies (or equally dark halos), so we should compare the theoretical prediction with large image separation side in CLASS data. In Fig.3, we take the NFW profile and compare the dependence on the cosmological models. The lensing probability is the highest for EdS model. This is due to the fact that the PS mass function is proportional to Ω_0 (see Eq.(17)) and the concentration parameter c is the highest (see Eq.(8)). In Fig.4, we show the lens model dependence for Λ model. Since there are no lenses for large image separations ($6'' \leq \theta \leq 15''$) in CLASS sample, the steeper inner profile ($\alpha > 1.5$) seems disfavored. However, it is preliminary, since we do not know whether the subsample by Marlow et al. is a fair sample.

We estimate the sensitivity of the lensing probability to the model parameters. Using Eq.(14,15) and the CLASS data with the magnification of total images, it is estimated around

$\alpha = 1, \sigma_8 = 1, \lambda_0 = 1 - \Omega_0 = 0.7, w = -1$

$$\left.\frac{\delta N_\theta}{N_\theta}\right|_{\theta=6''} \simeq 7.4\ \frac{\delta\alpha}{\alpha} + 5.7\ \frac{\delta c_{med}}{c_{med}} + 4.3\ \frac{\delta\sigma_8}{\sigma_8} - 5.7\ \frac{\delta\lambda_0}{\lambda_0} + 0.35\ \frac{\delta w}{w}, \tag{24}$$

$$\left.\frac{\delta N_\theta}{N_\theta}\right|_{\theta=12''} \simeq 7.3\ \frac{\delta\alpha}{\alpha} + 6.3\ \frac{\delta c_{med}}{c_{med}} + 6.1\ \frac{\delta\sigma_8}{\sigma_8} - 6.3\ \frac{\delta\lambda_0}{\lambda_0} + 0.27\ \frac{\delta w}{w}, \tag{25}$$

where w is the equation of state of dark energy ($w = -1$ for the cosmological constant) and a flat FRW model is assumed. Eqs.(24) and (25) indicate clearly that the lensing probability is very sensitive to the lens model parameters (α, c_{med}) as well as the cosmological parameters (λ_0, σ_8), but not sensitive to dark energy parameter (w). For example, in order to put constraint on λ_0 within $\mathcal{O}(10)\%$ accuracy, one needs to determine the inner profile α and the concentration parameter c with similar accuracy. The dispersion of concentration parameter c is about 0.2 (Jing 2000, Bullock *et al.* 2001). However, the current uncertainty in α is $\mathcal{O}(50)\%$ ($\alpha \sim 1 - 1.5$). Hence, it may be more useful to use the number of large image separation lenses to constrain the inner density profile α. Cosmological parameters λ_0 and σ_8 could be determined within $\mathcal{O}(10)\%$ by using CMB, SNIa and number count of clusters data (de Bernardis *et al.* 2001, Fan & Chiueh 2001). The sensitivity of the lensing probability to the model parameters was also estimated by Li & Ostriker (2000), but they assumed a single source at $z = 1.5$ and did not include the effect of magnification bias. So the detailed comparison may not be so meaningful. However, we note that the dependence on c and the cosmological constant parameter is slightly larger than that found by Li & Ostriker (2000).

In Fig.5, we show the effect of the scatter in N-body simulation on the image separation distribution. The dispersion of N_θ, σ_θ^2, is calculated by using the probability distribution function of c (Eq.(7)). We use the NFW profile for Λ model and compare the amplitude of the square of the dispersion σ_θ^2 with the predicted number of lenses N_θ. We find that the amplitude of σ_θ is comparable to or larger than N_θ, so the scatter of halo profiles strongly affect the lensing probability. When compared with Fig.3, we also find that the scatter is too large to distinguish the different cosmological models, even if the lens model (α) is fixed.

4. Prediction for Future Survey

With the current data, the constraints on the parameters are not sufficient. However, we expect that larger surveys currently underway such as the 2dF and SDSS detect a larger number of lenses. For example, the Sloan Digital Sky Survey (SDSS) plans a spectroscopic survey of 10^5 QSOs over π steradian brighter than $i' \sim 19$ at $z \leq 3.0$; at redshift between 3.0 and about 5.2, the limiting magnitude will be $i' \sim 20$ (York *et al.* 2000). In this section, we will make predictions for the SDSS.

Let $N_\theta d\theta$ be the expected number of lensed QSOs with image separation $\theta \sim \theta + d\theta$ within solid angle π in the sky. We use the QSOs luminosity function Φ_S for $z \geq 3$ in SDSS data (Fan *et al.* 2001), since Φ_S from 2dF redshift survey is known only for lower redshift QSOs ($z \leq 3$) (Boyle *et al.* 2000). Φ_S is fitted by a power-law,

$$\Phi_S(z_S, M_{1450}) = \Phi_S^* 10^{-0.4\{M_{1450}+26-\alpha(z_S-3)(\beta+1)\}}, \tag{26}$$

where M_{1450} is the absolute AB magnitude of the quasar continuum at $1450\mathring{A}$ in the rest frame. We assume $m_{i'} = m_{1450} + 0.7$. The fitting parameters for Λ model are given by (Fan *et al.* 2001)

$$(\Phi_S^*, \alpha, \beta) = (2.6 \times 10^{-7} h^3 \mathrm{Mpc}^{-3} \mathrm{mag}^{-1}, 0.75, -2.58). \tag{27}$$

Similarly, for lower redshift sources ($z \leq 3$) the QSO luminosity function (Eq.(19,20)) is used (Boyle *et al.* 2000). Then, using the QSO luminosity function Φ_S, $N_\theta(\theta)$ can be calculated as

$$\begin{aligned} N_\theta(\theta) &= \int_0^{z_{max}} dz \frac{dV_\pi}{dz} \int_{L_{lim}(z)}^{\infty} dL \, \frac{dP}{d\theta}(\theta, z, L) \Phi_S(z, L), \\ \frac{dV_\pi}{dz} &= \pi \frac{(1+z)^2 D(z)^2}{H(z)}, \end{aligned} \tag{28}$$

where $z_{max} = 5.2$ and $L_{lim}(z)$ is calculated from the limiting magnitude. In Fig.6, we show the predicted image separation distribution for SDSS. We use various lens model for Λ model. In this model, the number of QSOs is expected to be about 26,000. In Table 1, the expected number of large image separation lenses ($6'' \leq \theta \leq 30''$) is shown. We find that the ambiguity resulting from the treatment of magnification bias is not so large. From this table, we expect that the future SDSS data could set constraint on the inner density profile.

5. Summary and Discussion

We have examined the influence of the inner density profile of lenses on gravitational lens statistics carefully taking into account of the effect of magnification bias and the evolution and the scatter in halo profiles. We have estimated the sensitivity of the lensing probability to the inner density profile of lenses and to the cosmological constant. We have found that lensing probability is strongly dependent on the inner density profile as well as on the cosmological constant. We have also shown that magnification bias for the NFW is order of magnitude larger than that for SIS. There is an uncertainty in the treatment of magnification bias: fainter image should be detected in the survey, or the light from both the fainter and brighter images is initially unresolved in a single image and thus the total image should be detected. However, for NFW profile, difference between the magnification bias of the fainter

image and that of the total image is found to be only by factor of three. In any case, we should be careful about magnification bias which strongly depends on the lens profile. We have compared the predictions with the CLASS data and suggested that the steeper inner profile ($\alpha > 1.5$) seems disfavored. The absence or presence of large splitting events in larger surveys currently underway such as the 2dF and SDSS could set constraints on the inner density profile of dark halos.

Recently, using the arc statistics of gravitational lensing, various authors have examined the inner profile of dark halos (Bartelmann *et al.* 1998, Molikawa & Hattori 2000, Oguri, Taruya & Suto 2001). Comparing with the existing observational data, Molikawa & Hattori (2001) and Oguri, Taruya & Suto (2001) suggested that the steeper inner profile of dark halos ($\alpha > 1$ or even $\alpha > 1.5$) is favored. On the other hand, the absence of large images separations in QSOs multiple images in the CLASS sample constrains the inner profile and rather disfavors the steeper profile. Combining the arc statistics and the statistics of QSOs multiple image, we could narrow the allowed range of the inner profile of dark halos, or more interestingly both methods might exhibit discrepancy.

In any event, larger surveys will produce a lot of QSOs multiple images in near future and theoretical development especially concerning the uncertainties of various models will be expected. So we will get clues to the nature of dark matter.

We would like to thank Professor Yasushi Suto, Dr. Ryoichi Nishi for useful discussion and comments. One of the authors (RT) also thanks Dr. Atsushi Taruya and Dr. Masamune Oguri for useful comments. This work was supported in part by a Grant-in-Aid for Scientific Research (No.13740154) from the Japan Society for the Promotion of Science.

REFERENCES

Bartelmann, M. 1996, A&A, 313, 697

Bartelmann, M., Huss, A., Colberg, J.M., Jenkins, A. & Pearce, F.R. 1998, A&A, 330, 1

Bardeen, J.M., Bond, J.R., Kaiser, N. & Szalay, A.S. 1986, ApJ, 304, 15

Borriello, A. & Salucci, P. 2001, MNRAS, 323, 285

Boyle, B.J., Shanks, T. & Peterson, B.A. 1988, MNRAS, 235, 935

Boyle, B.J. *et al.* 2000 MNRAS, 317, 1014

Browne, I.W.A. & Myers, S.T. 2000, IAU Symposium 201, 47

Bullock, J.S. *et al.* 2001, MNRAS, 321, 559

Cen, R., Gott, J.R.,III, Ostriker, J.P. & Turner, E.L. 1994, ApJ, 423, 1

de Bernardis, P. *et al.* 2001, astro-ph/0105296

de Blok, W.J.G., McGaugh, S.S., Bosma, A. & Rubin, V.C. 2001, astro-ph/0103102

Dunlop, J.S. & Peacock, J.A. 1990, MNRAS, 247, 19

Dyer, C.C. & Roeder, R.C. 1973, ApJ, 180, L31

Einasto, J. & Einasto, M. 2000, Publ.Astron.Soc.Pac., 209, 360 (astro-ph/9909437)

Fan, X. *et al.* 2001, AJ, 121, 54

Fan, Z. & Chiueh, T. 2001, ApJ, 550, 547

Flores, R.A. & Primack, J.R. 1996, ApJ, 457, L5

Flores, R.A., Maller, A.H., & Primack, J.R. 2000, ApJ, 535, 555

Fox, D.C. & Pen, U-L. 2001, ApJ, 546, 35

Fukugita, M., Futamase, T., Kasai, M., & Turner, E.L. 1992, ApJ, 393, 3

Fukushige, T. & Makino 2001, ApJ, 557, 533

Helbig, P. 2000, astro-ph/0008197

Jing, Y.P. 2000, ApJ, 535, 30

Keeton, C.R. & Madau, P. 2001, ApJ, 549, L25

Keeton, C.R. 2001, astro-ph/0105200

Kitayama, T. & Suto, Y. 1996, ApJ, 469, 480

Kochanek, C.S. 1995, ApJ, 453, 545

Kochanek, C.S. 1996, ApJ, 466, 638

Kochanek, C.S. & White, M. 2001, astro-ph/0102334

Li, Li-Xin & Ostriker, P.J. 2000, astro-ph/0010432

Maoz, D. *et al.* 2000, ApJ, 486, 75

Marlow, D.R. *et al.* 2000, AJ, 119, 2629

Molikawa, K. & Hattori, M. 2000, astro-ph/0009343

Moore, B., Quinn, T., Governato, F., Stadel, J. & Lake, G. 1999, MNRAS, 310, 1147

Mortlock, D.J. & Webster, R.L. 2000, MNRAS, 319, 872

Myers, S.T. *et al.* 1995, ApJ, 447, L5

Nakamura, T.T. & Suto, Y. 1997, Prog. Theor. Phys., 97, 49

Narayan, R. & White, S.D.M. 1988, MNRAS, 231, 97p

Navarro, J.F., Frenk, C.S. & White, S.D.M. 1996, ApJ, 462, 563

Navarro, J.F., Frenk, C.S. & White, S.D.M. 1997, ApJ, 490, 493

Oguri, M., Taruya, A. & Suto, Y. 2001, astro-ph/0105248

Peebles, P.J.E. 1993, *Principles of Physical Cosmology*, (Princeton University Press, Princeton)

Phillips, P.M., Browne, I.W.A. Wilkinson, P.N. & Jackson, N.J. 2000, astro-ph/0011032

Porciani, O. & Madau, P. 2000, ApJ, 532, 679

Press, W.H. & Schechter, P. 1974, ApJ, 187, 425

Rees, M.J. & Ostriker, J.P. 1977, MNRAS, 179, 541

Rusin, D. & Tegmark, M. 2001, ApJ, 553, 709

Sasaki, S. & Takahara, F. 1993, MNRAS, 262, 681

Schneider, P. Ehlers, J. & Falco, E.E. 1992, *Gravitational Lenses*, (Springer-Verlag, New York)

Sugiyama, N. 1995, ApJS, 100, 281

Tomita, K. 1996, PASJ, 48, 265

Tomita, K. 1998, Prog.Theor.Phys., 100, 79

Tomita, K., Asada, H. & Hamana, T. 1999, Prog.Theor.Phys.Suppl., 133, 155

Turner, E.L., Ostriker, J.P. & Gott, J.R. 1984, ApJ, 284, 1

Tyson, J.A., Kochanski, G.P. & Dell'Antonio, I.P. 1998, ApJ, 498, L107

van den Bosch, F.C., Robertson, B.E., Dalcanton, J.J. & de Blok, W.J.G. 2000, AJ, 119, 1579

York, D.G. *et al.* 2000, AJ, 120, 1579

Wambsganss, J. *et al.* 1995, Science, 268, 174

Wambsganss, J., Cen, R. & Ostriker, J.P. 1998, ApJ, 494, 29

Wyithe, J.S.B., Turner, E.L. & Spergel, D.N. 2001, ApJ, 555, 504

	SIS	$\alpha = 1.5$	$\alpha = 1$	$\alpha = 0.5$
$N_\theta(6'' \leq \theta \leq 30'')$ μ total	197.5	31.0	7.3	1.6
μ fainter	37.5	10.9	2.4	0.43

Table 1: The expected number of large image separation lenses ($6'' \leq \theta \leq 30''$) for SDSS data for Λ model with magnification bias of the fainter image (bottom) and the total images (top). The total QSOs number is expected to be about 26,000.

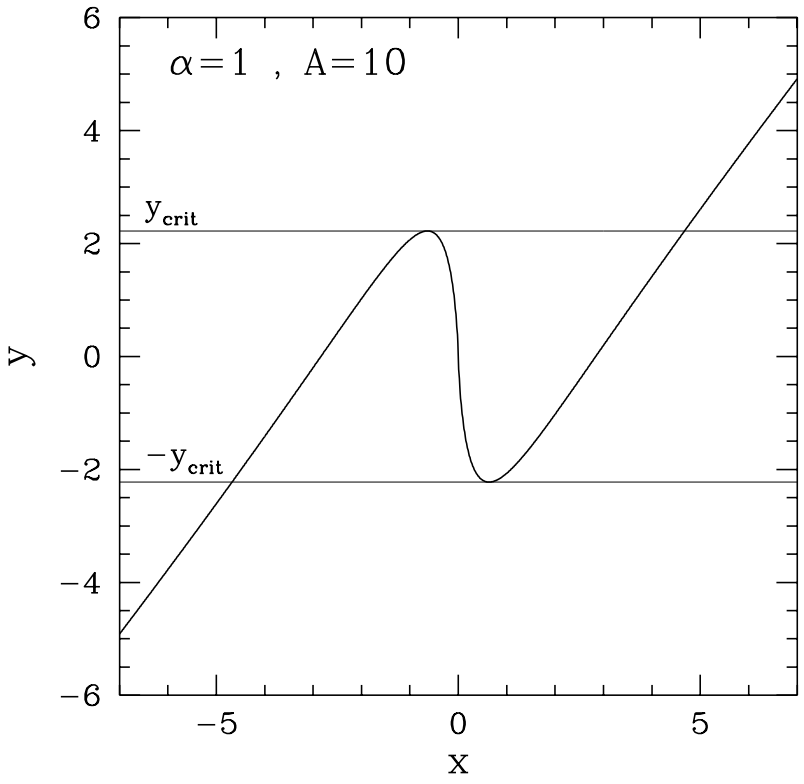

Fig. 1.— The lens equation for the NFW. The case with $A = 10$ is shown. The horizontal axis is x, which is the impact parameter normalized by a scale radius r_s in the lens plane; the vertical axis is y, which is the source position normalized by a scale radius r_s in the source plane. Multiple images are formed when $|y| \leq y_{crit}$.

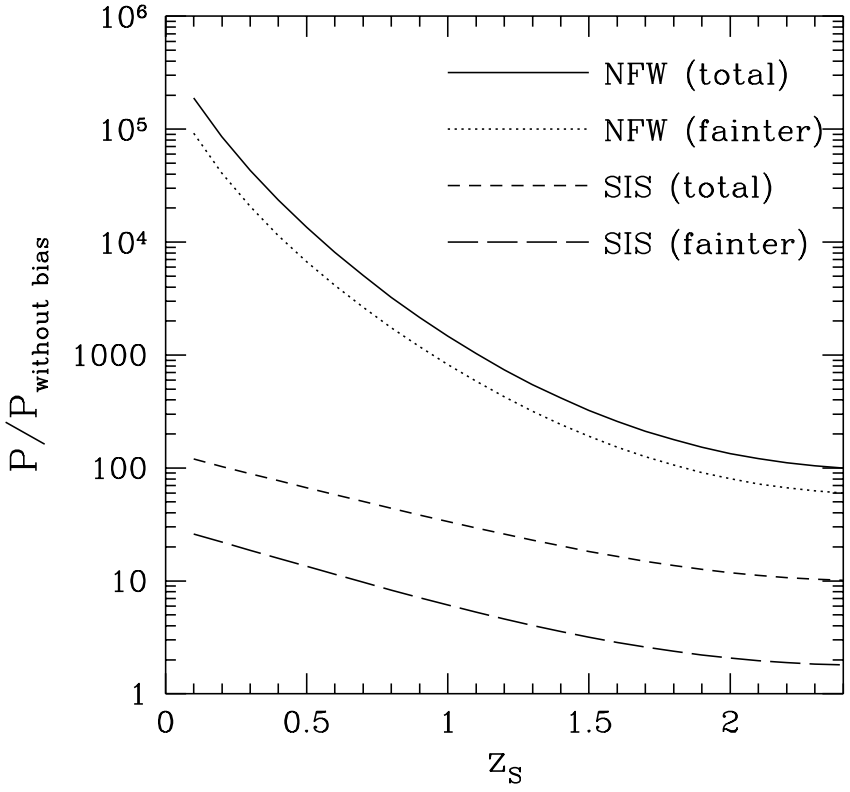

Fig. 2.— The amplitude of magnification bias for Λ model ($h = 0.7, \Omega_0 = 0.3, \lambda_0 = 0.7, \sigma_8 = 1.0$) with the absolute magnitude of a source being $M_B = -25.8$ mag. The horizontal axis is z_S, which is the source redshift; the vertical axis is a ratio lensing probability with the magnification bias to that without it. Image separation range $\theta \geq 0.3''$. The solid (dotted) line is the NFW profile for the case of the magnification of the total images (the fainter image). The short (long dashed) line is SIS for the case of the magnification of the total images (the fainter image).

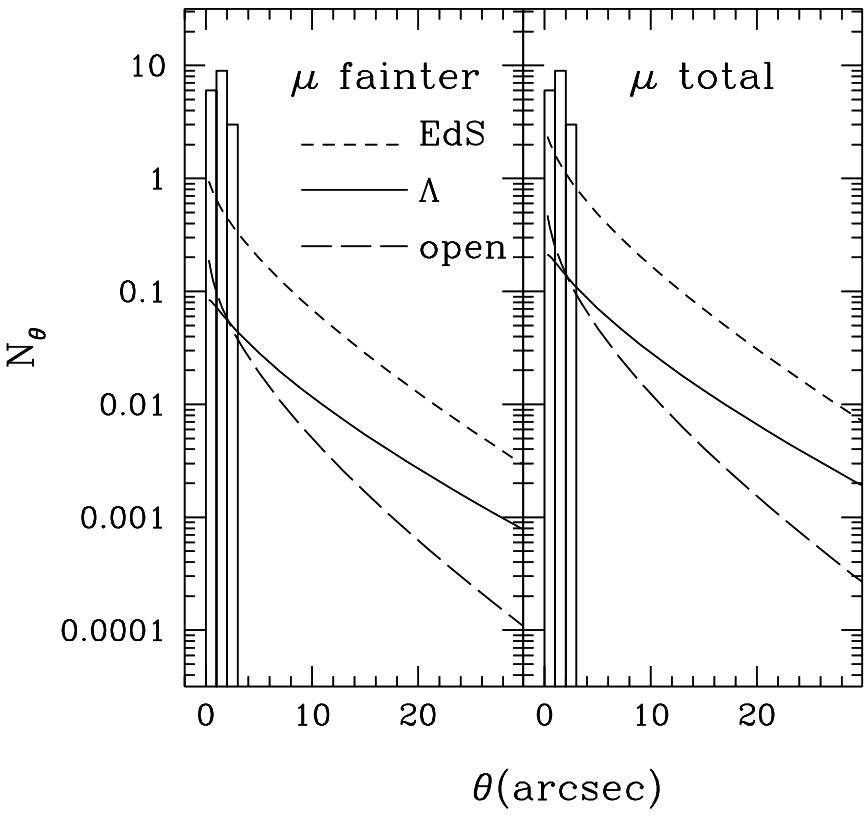

Fig. 3.— The distribution of image separations for the NFW lens model. The assumed cosmologies are EdS model(short-dashed: $h = 0.5, \Omega_0 = 1, \lambda_0 = 0, \sigma_8 = 0.67$), Λ model (solid: $h = 0.7, \Omega_0 = 0.3, \lambda_0 = 0.7, \sigma_8 = 1$) and open model(long-dashed: $h = 0.7, \Omega_0 = 0.3, \lambda_0 = 0, \sigma_8 = 0.85$). The left figure is for the selection condition in which fainter image should be detected in the survey, and the right figure is for the selection condition that the light from both the fainter and brighter images is initially unresolved in a single image. "μ total" is appropriate in the CLASS. The observational data from CLASS are shown by the histogram.

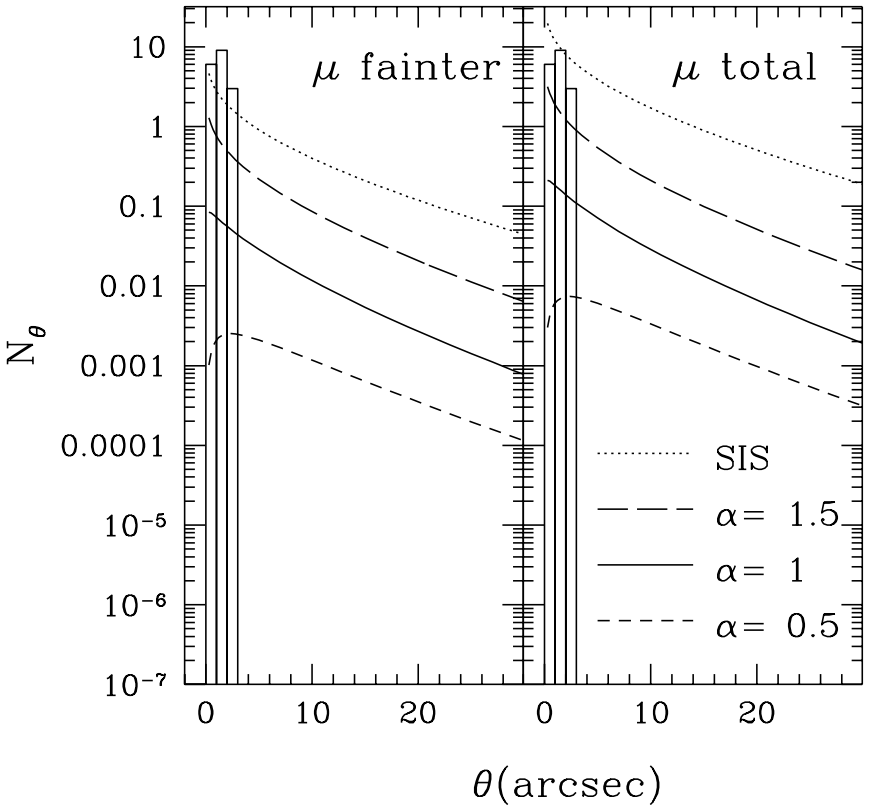

Fig. 4.— Same as Fig.3, but for various lens models (dotted: SIS, long-dashed: the generalized NFW with $\alpha = 1.5$, solid: NFW ($\alpha = 1$), short-dashed: the generalized NFW with $\alpha = 0.5$). Λ model is assumed for cosmology. The observational data from CLASS are shown by the histogram.

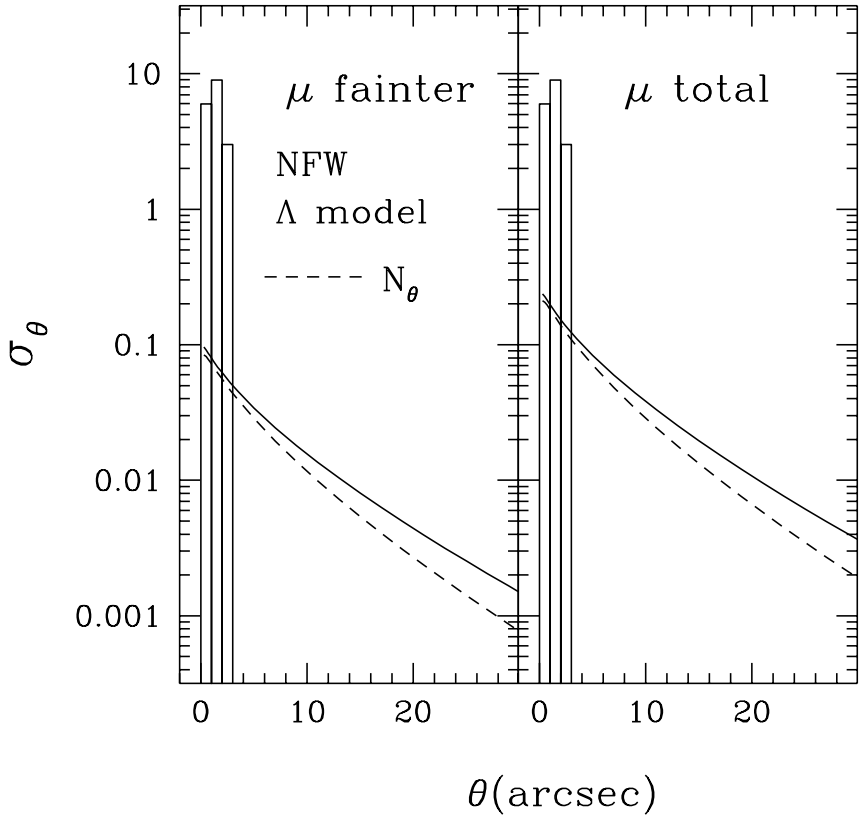

Fig. 5.— The dispersion of the predicted number of lenses caused by the scatter of halo profiles in N-body simulation. The solid line is the square of the dispersion (standard deviation), the dashed line is the averaged distribution of image separations. Λ model and the NFW profile ($\alpha = 1$) are assumed.

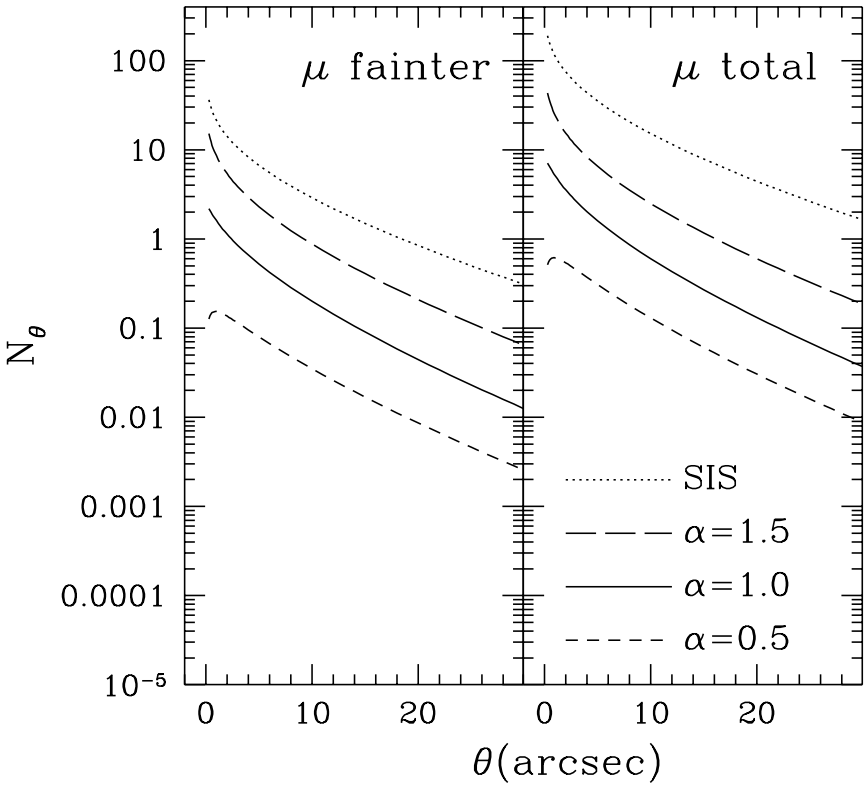

Fig. 6.— The image separation distribution expected for SDSS data for various lens models. Λ model is assumed for cosmology. The total QSOs number is estimated to be 26,000.